Analysis of Inter-system Bias Characteristics Between GPS/BDS and Influence on PPP

Yaqiong Huang(✉), Longping Zhang, Liang Yuan, XianCai Tian, and JunWei Zhang

Piesat Information Technology Co., Ltd., Beijing 100195, China
huangyaqiong@piesat.cn

Abstract. In GNSS multi-system fusion positioning, inter-system bias must first be considered. The analysis of the inter-system bias characteristics is helpful for the prediction and modeling of the inter-system basic, improving the precision and convergence speed of precise point positioning. This paper constructes GPS/BDS ionospheric-free combined PPP observation equation by considering ISB parameters. On this basis, the difference between BDS-2/GPS ISB and BDS-3/GPS ISB, the characteristics of BDS-2/BDS-3 ISB and its impact on PPP are analyzed. The results show that GPS/BDS ISB estimation by fusion of BDS-2 and BDS-3 observation data possesses the average characteristics, the estimation process is more stable, the positioning result accuracy is higher, and the convergence speed is faster. In the static state, the positioning accuracy is about 0.6 cm in N direction, about 0.9 cm in E direction, and about 1.4 cm in U direction. The convergence time is about 15 min. The BDS-2/BDS-3 ISB is within ± 10 ns, and the long- and short-term changes are stable, depending on the receiver type. Considering the ISB between BDS-2/BDS-3 systems can help improve positioning accuracy and convergence speed.

Keywords: Inter-system bias · Beidou navigation satellite system · Precise point positioning · Uncombined model · Long-term characteristics · Short-term characteristics

1 Introduction

Multi-constellation global navigation satellite system measurement data fusion can effectively improve the accuracy and reliability of navigation and positioning solutions, and inter system bias (ISB) is a key issue affecting system compatibility [1–3].

When using the Global Navigation Satellite System (GNSS) for positioning calculation, it is necessary to consider the difference between the coordinate base and the time base of each system [4]. There is only a slight difference in the flatness of the reference ellipsoid between the WGS-84 coordinate system used by GPS (Global Positioning System) and the CGCS2000 Chinese geodetic coordinate system used by the Beidou navigation satellite system, and the effect of flatness changes on the latitude, longitude, and height of the earth is in mm Level, can be ignored in the precision point positioning solution [5]. In GNSS multi-system data fusion, the time reference is usually unified to

C. Yang and J. Xie (Eds.): *China Satellite Navigation Conference (CSNC 2022) Proceedings*, LNEE 910, pp. 75–88, 2022.
https://doi.org/10.1007/978-981-19-2576-4_8

GPS time, but the difference in the reference clock satellites selected by different systems in the calculation process will still lead to differences in the satellite clock difference reference of each system, and the modulation of the navigation signal of each satellite The large differences in methods, receiver hardware, and firmware versions cause systematic differences in the hardware delay time of different navigation systems within the multi-mode receiver. The difference between the satellite clock reference difference of different systems and the receiver hardware delay error is the ISB, and its specific form can be expressed as the difference of the receiver clock difference between different systems including no ionospheric combined hardware delay [6–8].

The fusion positioning of Beidou and GPS first needs to consider the ISB. In recent years, many scholars have carried out multi-dimensional research on ISB between Beidou-2 (denoted as BDS-2) and GPS, including the estimation method and characteristic analysis [9–14]. At the end of 2018, the Beidou-3 system was basically deployed, and related research on the ISB between the Beidou-3 (denoted as BDS-3) and GPS was gradually launched [15, 16]. Liu et al. analysed the size and time-varying characteristics of GPS/BDS-3 ISB between receivers of the same type, and showed that the influence of the same type of receiver BDS-3/GPS ISB on the relative positioning of the tight combination can be ignored [17]. However, there are few studies on the difference between BDS-2/GPS ISB and BDS-3/GPS ISB.

On June 23, 2020, the global networking work of the Beidou-3 system is completed, it provided basic conditions, for the research of BDS-2/BDS-3 ISB [18]. Song et al. analysed the ISB variation characteristics between BDS-2 and BDS-3 on un-overlapping frequencies [19]. The results show that there is an ISB between BDS-2 and BDS-3 of non-overlapping frequencies, and it is related to the type of tracking station receiver. In PPP should consider the ISB. However, the BDS-2/BDS-3 ISB between overlapping frequencies was not analysed. He analysed the daily stability of ISB between the overlapping frequencies of BDS-2 and BDS-3 [20]. The results show that the changes within the day are stable and the magnitude is small, and the impact can be ignored when the positioning accuracy is not high. However, only the daily stability was analysed, and no in-depth study was carried out on more characteristics of the same frequency BDS-2/BDS-3 ISB.

This paper builds a GPS/BDS ionospheric-free combination PPP model that takes into account ISB parameters on the basis of the ionospheric-free combination model. On this basis, the difference between BDS-2/GPS ISB and BDS-3/GPS ISB, BDS-2/BDS-3 ISB magnitude, long-term and short-term characteristics, relationship with the receiver and its impact on PPP positioning performance are analysed.

2 Constructing GPS/BDS PPP Model Considering ISB Parameters

2.1 Original GPS/BDS PPP Ionospheric-Free Combined Model

The ionospheric-free combined observation equation based on the dual-frequency pseudorange and carrier phase observations is:

$$P_{IF} = \rho + c\left(dt_r - dt^s\right) + T + M_{p_{IF}} + \varepsilon_{p_{IF}} \tag{1}$$

$$L_{IF} = \rho + c\left(dt_r - dt^s\right) + T + \lambda_{IF} N_{IF} + M_{L_{IF}} + \varepsilon_{L_{IF}} \tag{2}$$

Among them, $\rho = \sqrt{(x_s - x_r)^2 + (y_s - y_r)^2 + (z_s - z_r)^2}$ is the geometric distance between the receiver and the satellite; (x_s, y_s, z_s) represents the satellite location; (x_r, y_r, z_r) represents the receiver location; P_{IF} represents the ionosphere-free combined pseudorange observations; L_{IF} represents the ionosphere-free combined carrier phase observations; dt_r represents the receiver clock error that absorbs the receiver pseudorange deviation; dt^s represents the satellite clock error that absorbs the satellite pseudorange deviation; T represents the tropospheric delay; λ_{IF} represents the frequency wavelength of non-ionospheric combined; N_{IF} represents un-ionospheric combined ambiguity including hardware delay and initial phase deviation; M , ε denote the multipath effect error and other residual errors that are not parameterized and modeled, respectively; c represents speed of light. All units in the above equation are meters (m).

Application the precision products, the non-ionospheric combined observation equation of GPS/BDS-2/BDS-3 can be expressed as:

$$P_{IF}^G = \rho^G + cdt_r^G + T^G + M_{p_{IF}}^G + \varepsilon_{p_{IF}}^G \tag{3}$$

$$L_{IF}^G = \rho^G + cdt_r^G + T^G + \lambda_{IF}^G N_{IF}^G + M_{L_{IF}}^G + \varepsilon_{L_{IF}}^G \tag{4}$$

$$P_{IF}^{C2} = \rho^{C2} + cdt_r^{C2} + T^{C2} + M_{p_{IF}}^{C2} + \varepsilon_{p_{IF}}^{C2} \tag{5}$$

$$L_{IF}^{C2} = \rho^{C2} + cdt_r^{C2} + T^{C2} + \lambda_{IF}^{C2} N_{IF}^{C2} + M_{L_{IF}}^{C2} + \varepsilon_{L_{IF}}^{C2} \tag{6}$$

$$P_{IF}^{C3} = \rho^{C3} + cdt_r^{C3} + T^{C3} + M_{p_{IF}}^{C3} + \varepsilon_{p_{IF}}^{C3} \tag{7}$$

$$L_{IF}^{C3} = \rho^{C3} + cdt_r^{C3} + T^{C3} + \lambda_{IF}^{C3} N_{IF}^{C3} + M_{L_{IF}}^{C3} + \varepsilon_{L_{IF}}^{C3} \tag{8}$$

Among them, the superscripts G, C2, and C3 indicate GPS, BDS-2, and BDS-3, respectively.

2.2 Combined GPS/BDS PPP Ionospheric-Free Combined Model Considering ISB Parameters

In order to ensure the same definition of the receiver clock difference between GPS, BDS-2, and BDS-3, use the GPS receiver clock error as a reference to introduce the ISB parameters, after introduction of the ISB the dual-frequency ionospheric-free combined observation equation of the BDS-2 and BDS-3 can be expressed as:

$$P_{IF}^{C2} = \rho^{C2} + cdt_r^G + cISB_{G,C2} + T^{C2} + M_{p_{IF}}^{C2} + \varepsilon_{p_{IF}}^{C2} \tag{9}$$

$$L_{IF}^{C2} = \rho^{C2} + cdt_r^G + cISB_{G,C2} + T^{C2} + \lambda_{IF}^{C2} N_{IF}^{C2} + M_{L_{IF}}^{C2} + \varepsilon_{L_{IF}}^{C2} \tag{10}$$

$$P_{IF}^{C3} = \rho^{C3} + cdt_r^G + cISB_{G,C3} + T^{C3} + M_{p_{IF}}^{C3} + \varepsilon_{p_{IF}}^{C3} \tag{11}$$

$$L_{IF}^{C3} = \rho^{C3} + cdt_r^G + cISB_{G,C3} + T^{C3} + \lambda_{IF}^{C3} N_{IF}^{C3} + M_{L_{IF}}^{C3} + \varepsilon_{L_{IF}}^{C3} \tag{12}$$

Among them,

$$cISB_{G,C2} = cdt_r^{C2} - cdt_r^G \tag{13}$$

$$cISB_{G,C3} = cdt_r^{C3} - cdt_r^G \tag{14}$$

$ISB_{G,C2}$, $ISB_{G,C3}$ represents ISB between GPS and BDS-2 and ISB between GPS and BDS-3, respectively.

Record the ISB between BDS-2 and BDS-3 as $ISB_{C2,C3}$, has:

$$c \cdot ISB_{C2,C3} = c \cdot ISB_{G,C3} - c \cdot ISB_{G,C2} \tag{15}$$

2.3 Parameter Estimation of GPS/BDS PPP Ionospheric-Free Combined Model Considering ISB Parameters

When m satellites are observed at epoch i and station r, the estimable parameter $\mathrm{X}(i)$ and the design matrix $\mathrm{A}(i)$ can be expressed as:

$$\underset{(5+2m)\times 1}{\mathrm{X}(i)} = \begin{bmatrix} \Delta \mathrm{X} & \Delta cdt_r & \Delta\rho_{zd} & c \cdot ISB_{G,C3}^k & \Delta N_{r,IF}^k \end{bmatrix}^T \tag{16}$$

$$\underset{4m\times(5+2m)}{\mathrm{A}(i)} = \begin{bmatrix} \mathrm{B}(i) & 0 & 0 \\ \mathrm{B}(i) & 0 & \Gamma_{IF} \\ \mathrm{B}(i) & I_m & 0 \\ \mathrm{B}(i) & I_m & \Gamma_{IF} \end{bmatrix}, \underset{m\times 5}{\mathrm{B}(i)} = \begin{bmatrix} -\mu^1 & 1 & mf_r^1(i) \\ \vdots & \vdots & \vdots \\ -\mu^m & 1 & mf_r^m(i) \end{bmatrix} \tag{17}$$

Among them, ρ_{zd} indicates the tropospheric delay parameter in the direction of the zenith of the station; mf_r represents the tropospheric delay projection function; Γ_{IF} represents a diagonal matrix with m-dimensional diagonal elements λ_{IF}; $-\mu = \begin{bmatrix} \frac{x^s - x_0}{\rho_0} & \frac{y^s - y_0}{\rho_0} & \frac{z^s - z_0}{\rho_0} \end{bmatrix}$ is the three-dimensional position of the receiver; $\Delta \mathrm{X} = \begin{bmatrix} \Delta x & \Delta y & \Delta z \end{bmatrix}^{\mathrm{T}}$ linearization parameter.

3 Experimental Data Selection and Experimental Settings

Four different receiver types, two stations for each receiver type, and DOY181–204 (24 days in total) observation data in 2020 for the experiments are selected in this article. The specific station information is listed in Table 1. In this experiment, the true value of the station coordinate is fixed as a constant, the receiver clock error is estimated as white noise, the ambiguity parameter is fixed as a constant, and when a cycle slip occurs, it is fixed again. Other information such as error correction model selection, filtering method, use of data files, etc. are shown in Table 2.

Table 1. Station information is used in the experiment

Station name	Latitude/Longitude/(°)	Receiver type
AJAC	8.8,41.9	SEPT POLARX5
IISC	77.6,13.0	SEPT POLARX5
GANP	20.3,49.0	TRIMBLE ALLOY
JFNG	114.5,30.5	TRIMBLE ALLOY
CUSV	100.5,13.7	JAVAD TRE_3 DELTA
HUEG	7.6,47.8	JAVAD TRE_3 DELTA
NYAL	11.9,78.9	TRIMBLE NETR9
SOLO	159.9,-9.4	TRIMBLE NETR9

Table 2. Data processing method

Type	Method
Filter processing method	Forward filtering
Satellite cut-off angle	10 (°)
Tropospheric correction	The function model adopts the Saastamoinen model, the mapping function adopts the Neal Mapping Function (NMF), the prior model and the parameter estimation are combined
Receiver clock offset	White noise estimation
Cycle slip detection and repair	Combined observations of MW and GF
Orbital clock difference	IGS precision products, 15 min orbit sampling interval, 30 s clock difference sampling interval
Antenna correction	Use igs14.atx file
Ambiguity	Piecewise constant estimation
Decision convergence	Accuracy is better than 0.1 m for 20 consecutive epochs
Reference	IGS weekly solution coordinates
Coordinate parameters	Static positioning uses a constant model, dynamic positioning is a white noise model
Tidal effect	Model corrections for solid tides, ocean tides, and extreme tides
Relativistic effect	Correction of Relativistic Clock Error and Gravitational Field Delay Model

4 The Difference Between BDS-2/GPS ISB and BDS-3/GPS ISB

Designing plan analyzes the difference between BDS-2/GPS ISB and BDS-3/GPS ISB, as shown in Table 3. L1 and L2 frequency observation data of GPS are used, BDS-2,

BDS-3 B1I, B3I frequency observation data of BDS are used, B1I and B3I frequency observation data of BDS-2 are used; B1I and B3I frequency observation data of BDS-3 are used; ISB estimates using the 30-min piecewise constant method.

Table 3. ISB estimation scheme between GPS/BDS or GPS/BDS-2or GPS/BDS-3

Plan	Describe	ISB estimation method
ISB(G/C)	Estimated ISB between GPS and BDS	30 min piecewise constant
ISB(G/C2)	Estimated ISB between GPS and BDS-2	30 min piecewise constant
ISB(G/C3)	Estimated ISB between GPS and BDS-3	30 min piecewise constant

Good positioning result is prerequisite for estimating ISB. Statistics of G/C, G/C2, G/C3 static PPP positioning accuracy and convergence time are shown in Fig. 1. It can be seen from Fig. 1 that G/C, G/C2, and G/C3 static PPP all have good positioning accuracy. Among them, G/C has higher positioning accuracy (N direction is about 0.6 cm, E direction is about 0.9 cm, U direction is about 1.4 cm) and less convergence time (about 15 min).

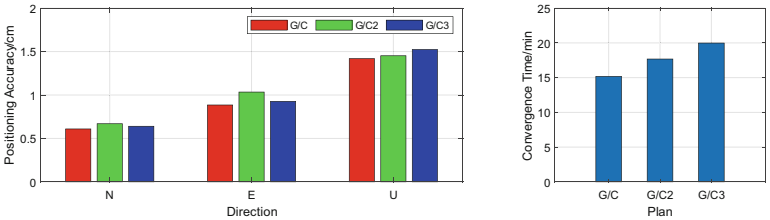

Fig. 1. Static PPP positioning accuracy and convergence time of G / C, G / C2 and G / C3

Three schemes ISB estimation sequence diagrams of each station are similar. Taking IISC station DOY184 as an example (Fig. 2), it can be seen that the G/C ISB sequence is always between G/C2 and G/C3, and is always in the middle position. Analysis ISB(G/C) = (ISB(G/C2) + ISB(G/C3))/2. Count the difference between ISB(G/C) and [(ISB(G/C2) + ISB(G/C3)/2] (denoted as dISB) in DOY181–204 at each station, as shown in Table 4.

It can be seen from Table 4 that dISB is between 0 and 3 ns, the average value is about 0.23 ns, and the error is at the centimeter level. Compared to GPS/BDS ISB, the difference between BDS-2/GPS ISB and BDS-3/GPS ISB is very small. Explain that when analyzing GPS/BDS ISB, BDS-2 and BDS-3 can be directly fused, and there is no need to discuss BDS-2 and BDS-3 separately. And fusion of BDS-2 and BDS-3 for GPS/BDS ISB estimation has obvious advantages: First, the number of satellites is larger, the solution is more stable, and the stability of the estimation process is of great significance to

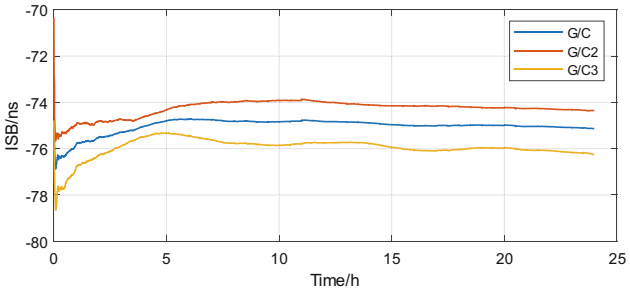

Fig. 2. IISC station DOY184 ISB estimation sequence diagram

Table 4. Minimum, maximum and mean value of dISB

Station name	MIN/ns	MAX/ns	AVG/ns
AJAC	0.3	0.9	0.55
IISC	0.07	0.37	0.21
GANP	0.34	1.24	0.79
JFNG	0.11	0.7	0.39
CUSV	0.52	1.33	0.86
HUEG	1.34	2.79	2.06
NYAL	0.02	0.23	0.09
SOLO	0.04	0.27	0.13
ALL	0.02	2.79	0.23

ISB forecasting and modeling; Second, ISB (G/C) is always between ISB (G/C2) and ISB (G/C3), with the characteristics of averaging the two; Third, from the positioning result statistics chart 1, the positioning accuracy is higher and the convergence speed is faster.

5 Analysis of ISB Characteristics Between BDS-2 and BDS-3 and Influence on PPP

Use ISB(C2/C3) = ISB(G/C3)-ISB(G/C2) to analyze the characteristics of BDS-2/BDS-3 ISB and its influence on static and dynamic PPP.

5.1 BDS-2/BDS-3 ISB Characteristic Analysis

5.1.1 Short-Term Characteristics

The daily ISB estimation sequence diagrams of each station are similar. Taking DOY181 as an example (Fig. 3), it can be seen that the single-day ISB estimate of each station

is relatively small. AJAC, IISC, JFNG, NYAL is about −2 ns; SOLO, GANP is about 4 ns; CUSV is about 6 ns; HUEG is about 8 ns. It can be seen that the ISB of the same frequency BDS-2/BDS-3 is relatively small, within ± 10 ns, the error of the distance is about 3 m, which needs to be considered in precise point positioning.

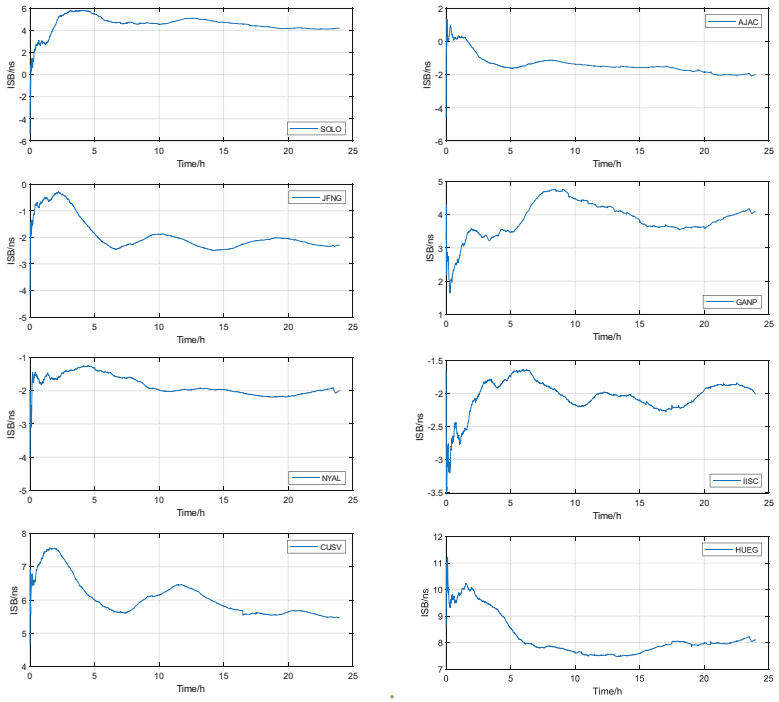

Fig. 3. ISB sequence of stations in DOY181

Further analyze the intraday stability of BDS-2/BDS-3 ISB. Take DOY203 as an example, draw a single-day ISB change chart, as shown in Fig. 4. The minimum, maximum, and average values of the ISB single-day change STD are counted, as shown in Table 5.

It can be seen from Fig. 4 and Table 5 that the ISB changes of each station in a single day are stable within ± 2 ns. The minimum value of STD is 0.18 ns, the maximum value is 1.82 ns, and the average value is about 0.62 ns.

5.1.2 Long-Term Characteristics

Plotting the ISB mean value sequence diagram (Fig. 5) shows that the daily ISB mean value difference of each station is small. According to the statistics of the mean STD of the ISB, the STD of the GANP station is the largest, about 0.78 ns, and the STD of the IISC station is the smallest, about 0.29 ns. The average STD of the eight stations is about 0.49 ns. It can be seen that the long-term changes of BDS-2/BDS-3 ISB are stable, and

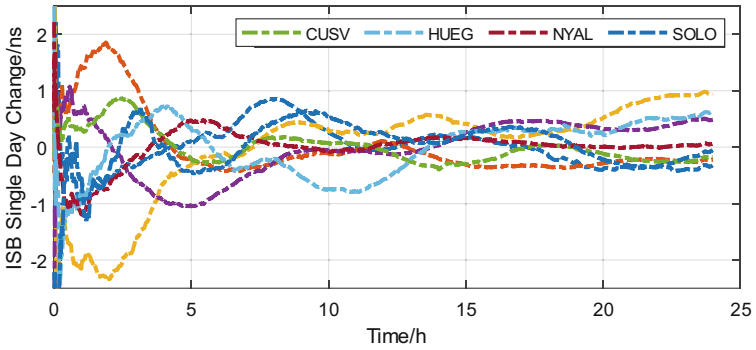

Fig. 4. Single day change of ISB at each station of DOY203

Table 5. Minimum, maximum and mean value of single day STD of ISB

Station name	MIN/ns	MAX/ns	AVG/ns
AJAC	0.39	1.54	0.80
IISC	0.21	1.43	0.46
GANP	0.43	1.43	0.73
JFNG	0.30	1.74	0.58
CUSV	0.20	0.86	0.49
HUEG	0.57	1.82	0.97
NYAL	0.18	0.67	0.32
SOLO	0.33	0.99	0.58
ALL	0.18	1.82	0.62

the STD is about 0.5 ns. This feature is conducive to BDS-2/BDS-3 ISB modeling and forecasting for a longer time.

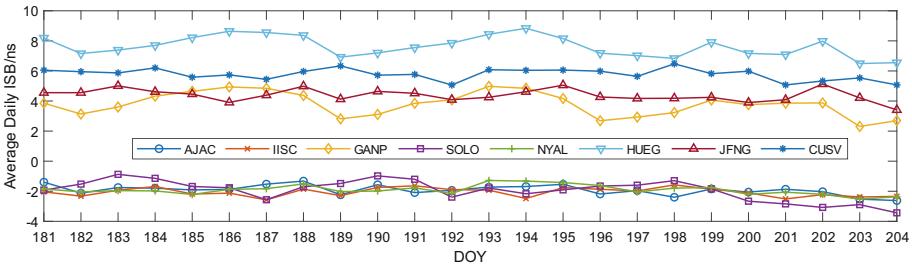

Fig. 5. Daily ISB mean sequence of each station

5.1.3 Relationship with Receiver

Count the difference in the average ISB value of a single day among the same type of receivers, as shown in Table 6. It can be seen that the ISB difference between receivers of the same type is small, the minimum is about 0.01 ns, the maximum is about 3.11 ns, and the average is about 0.89 ns.

Table 6. Minimum, maximum and mean value of single day ISB mean value difference between receivers of the same type

Station name	MIN/ns	MAX/ns	AVG/ns
AJAC- IISC	0.02	1.05	0.32
GANP- JFNG	0.01	1.90	0.82
CUSV- HUEG	0.36	3.11	1.86
NYAL- SOLO	0.03	1.08	0.54

Count the difference of the average single-day ISB between different types of receivers, as shown in Table 7. It can be seen that ISB is closely related to the type of receiver. Among them, AJAC and GANP (between SEPT POLARX5 and TRIMBLE ALLOY receivers), AJAC and CUSV (between SEPT POLARX5 and JAVAD TRE_3 DELTA receivers), GANP and NYAL (between TRIMBLE ALLOY and TRIMBLE NETR9 receivers), CUSV and NYAL (between JAVAD TRE_3 DELTA and TRIMBLE NETR9 receivers) The average single-day ISB difference is 5.71 ns, 7.70 ns, 5.70 ns, and 7.69 ns, respectively, which are quite different; while AJAC and NYAL (between SEPT POLARX5 and TRIMBLE NETR9 receivers), GANP and CUSV (between TRIMBLE ALLOY and JAVAD TRE_3 DELTA receivers), the average value of the ISB difference in a single day is 0.25 ns and 1.99 ns, respectively, and the difference is small. Note: Except for the small difference in ISB between SEPT POLARX5 and TRIMBLE NETR9 receivers, TRIMBLE ALLOY and JAVAD TRE_3 DELTA receivers, the ISB differences between other types of receivers are relatively large.

Table 7. Minimum, maximum and mean value of single day ISB mean value difference between receivers of the different type

Station name	MIN/ns	MAX/ns	AVG/ns
AJAC-GANP	4.67	6.81	5.71
AJAC-CUSV	6.94	8.87	7.70
AJAC-NYAL	0.00	0.61	0.25
GANP-CUSV	0.60	3.52	1.99
GANP-NYAL	4.31	6.86	5.70
CUSV-NYAL	7.13	8.36	7.69

5.2 The Influence of ISB Between BDS-2 and BDS-3 on PPP

Designing plan analyzes the impact of BDS-2/BDS-3 ISB on PPP. Option 1: Fuse the observation data of BDS-2 and BDS-3 without considering BDS-2/BDS-3 ISB; Option 2: Fuse the observation data of BDS-2 and BDS-3, consider BDS-2/ BDS-3 ISB.

Statistics of DOY181–204 static and imitation dynamic positioning results and convergence time of each station in 2020 are shown in Fig. 6 (static) and Fig. 7 (imitation dynamic). Taking the IGS weekly solution coordinates as the true value, the constant model is used for static positioning, the white noise model is used for imitation dynamic positioning, and the convergence is judged by the method that the accuracy is better than 0.1 m for 20 consecutive epochs.

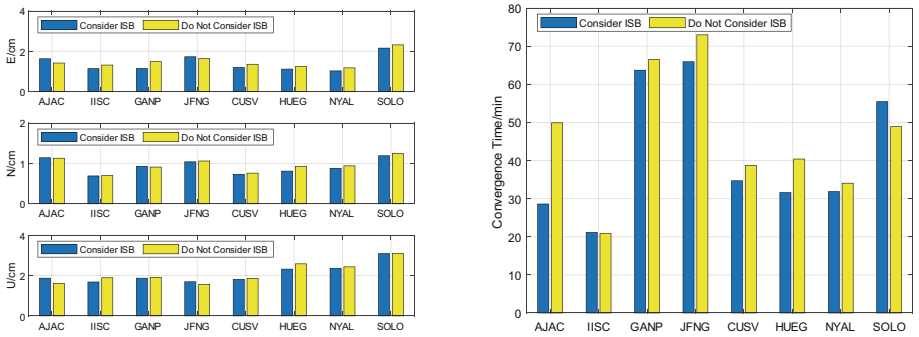

（a）Positioning accuracy of each station　　（b）Convergence time of each station

Fig. 6. Doy181–204 static positioning results and convergence time

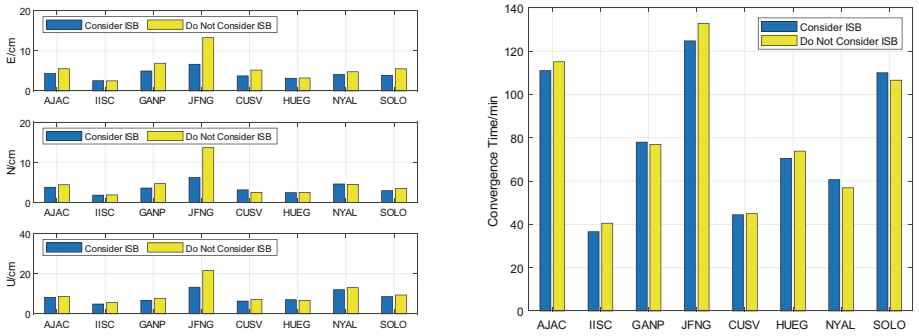

（a）Positioning accuracy of each station　　（b）Convergence time of each station

Fig. 7. Doy181–204 simulated dynamic positioning results and convergence time

It can be seen from Fig. 6 and Fig. 7 that when ISB is considered, the positioning accuracy is higher and the convergence speed is faster. Taking the pseudo-dynamic statistical results of the JFNG station as an example, the positioning accuracy is improved

by about 7.5 cm, or 46%; taking the static statistical results of the AJAC station as an example, the convergence time is shortened by about 20 min, or 43%. Among the specific stations, the IISC station has the highest positioning accuracy and the fastest convergence speed in both static and imitation dynamics. The positioning results of SOLO and JFNG stations are poor. The SOLO station has the lowest positioning accuracy when it is static, and the JFNG station has the lowest positioning accuracy and the slowest convergence speed when it is dynamic.

Statistics of the static and imitation dynamic average positioning accuracy and convergence time of the eight stations are shown in Table 8.

It can be seen from Table 8 that when the ISB is static, the positioning accuracy in the E direction is improved by about 6.7%, in the N direction is improved by about 3.1%, in the U direction is improved by about 1.4%, and the convergence time is improved by about 10.6%; when the ISB is dynamic, the positioning accuracy in the E direction is improved by about 28.8%, in the N direction is improved by about 24.5%, in the U direction is improved by about 16.2%, and the convergence time is improved by about 1.8%.

In Beidou navigation satellite system, in static, the positioning accuracy in the N direction is about 1 cm, with an average of millimeter level; in the E direction is about 1.5 cm; in the U direction is about 2 cm; and the convergence time is about 45 min. In imitates dynamic, the positioning accuracy in the N direction is about 4 cm; in the E direction is about 5 cm; in the U direction is about 9 cm; and the convergence time is about 80 min.

Table 8. Average positioning accuracy and convergence time of eight stations

Motion state	ISB plan	Positioning accuracy */cm*			Convergence time */min*
		E	N	U	
static	Do not consider ISB	1.50	0.96	2.12	46.53
	Consider ISB	1.40	0.93	2.09	41.62
Imitation dynamic	Do not consider ISB	5.87	4.70	10.03	80.97
	Consider ISB	4.18	3.55	8.41	79.50

6 Conclusion

Based on the ionospheric combination model, this paper constructs the GPS/BDS ionospheric combination PPP observation equation that takes into account the ISB parameters. Design experiments to analyze the differences between BDS-2/GPS ISB and BDS-3/GPS ISB, the characteristics of BDS-2/BDS-3 ISB under the condition of the same frequency observation data and its influence on PPP. The results show that the results of GPS/BDS ISB estimation by fusion of BDS-2 and BDS-3 observation data possess

average characteristics, and the estimation process is more stable, the positioning result accuracy is higher, and the convergence speed is faster.

The BDS-2/BDS-3 ISB is within ± 10ns, which is converted into a distance error of about 3m. This error needs to be considered in high-precision positioning. The BDS-2/BDS-3 ISB in short-term change is stable, within ± 2 ns, the average ISB change in a single day is about 0.62 ns. The BDS-2/BDS-3 ISB in long-term change is stable, and the STD is about 0.5 ns, which is conducive to long-term modeling and forecasting. The ISB difference between similar receivers is small, and the ISB difference between different types of receivers is relatively large, indicating that ISB is closely related to the receiver type.

Considering the ISB between BDS-2/BDS-3 can help improve positioning accuracy and convergence speed. In the static state, the positioning accuracy in the E direction, N direction and U direction are increased by about 6.7%, 3.1% and 1.4%, respectively. The convergence time is increased by about 10.6%. When imitating dynamics, the positioning accuracy in the E direction, N direction and U direction are increased by about 28.8%, 24.5% and 16.2%, respectively. The convergence time is increased by about 1.8%.

Thanks. Thanks to iGMAS and MGEX for providing GNSS data.

References

1. Yang, Y.X.: Concepts of comprehensive PNT and related key technologies. Acta Geodaetica et Cartographica Sinica **45**(5), 505–510 (2016)
2. Yang, Y.X.: Progress, contribution and challenges of compass/Beidou satellite navigation system. Acta Geodaetica et Cartographica Sinica **39**(1), 1–6 (2010)
3. Yang, Y., Mao, Y., Sun, B.: Basic performance and future developments of BeiDou global navigation satellite system. Satellite Navig. **1**(1), 1–8 (2020). https://doi.org/10.1186/s43020-019-0006-0
4. Cai, C.S., Li, Z.H., Zhang, X.H.: Study of calibration method of GPS satellite and receiver instrumental biases. Bulletin Surveying Mapp. **4**, 15–16 (2002)
5. Yuan, Y.B., Zhang, B.C., Li, M.: Precise estimation and characteristic analysis of multi-GNSS receiver differential code biases. J. Wuhan Univ. Inf. Sci. Ed. **43**(12), 2106–2111 (2018)
6. Gu, S.Z., Shi, C., Dang, Y.M., et al.: ISB Analysis and function model design in the real-time BDS/GPS clock estimation. Bulletin Surveying Mapp. **0**(1), 22–27 (2018)
7. Guan, J.N., Zhang, T., Liu, Z.K.: Real-time estimation and analysis of GNSS satellite clock. Eng. Surveying Mapp. **29**(01), 14–18+26 (2020)
8. Wen, H., Pan, S.G., Gao, W., Zhao, Q.: Accuracy analysis of GPS / BDS /Galileo/QZSS pseudo-range differential positioning considering pseudo-range differential inter-system bias corrections. Eng. Surveying Mapp. **29**(4), 15–20 (2020)
9. Chen, J.P., Xiao, P., Zhang, Y.Z., et al.: (2013) GPS/GLONASS System Bias Estimation and Application in GPS/GLONASS Combined Positioning. in China Satellite Navigation Conference (CSNC). In: Proceedings Lecture Notes in Electrical Engineering. vol. 244(1) pp. 323–333 (2013)
10. Dang, Y.M., Zhang, L.P., Chen, J.Y.: ISB/IFB estimation and characteristic analysis with multi-GNSS precise orbit determination. J. Wuhan Univ. Inf. Sci. Ed. **043**(012), 2079–2084 (2018)
11. Deng, Y.F., Guo, F., Ren, X.D., et al.: Estimation and analysis of multi-GNSS observable-specific code biases. GPS Solutions **25**(3), 1–13 (2021)

12. Sui, X., Shi, C., Xu, A.G., Yushi, H.: The stability of GPS/BDS inter-system biases at the receiver end and its effect on ambiguity resolution. J. Wuhan Univ. Inf. Sci. Ed. **43**(2), 175–182 (2018)
13. Wang, J., Yang, Y.X., Zhang, Q., et al.: Analysis of Inter-system bias in multi-GNSS precise point positioning. J. Wuhan Univ. Inf. Sci. Ed. **44**(04), 4–10 (2019)
14. Yang, Y.X., Gao, W.G., et al.: Introduction to BeiDou-3 navigation satellite system. J. Inst. Navig. **66**(1), 7–18 (2019)
15. Torre, A.D., Caporali, A.: An analysis of intersystem biases for multi-GNSS positioning. GPS Solutions **19**(2), 297–307 (2015)
16. Zhang, L.P., Xu, J.Y., Yu, H.Z., et al.: Unification of Multi-GNSS Bias Reference and Parameter Optimization of ISB/IFB Random Model. In: China Satellite Navigation Conference. Springer, Singapore, (2020)
17. Liu, C.H., Chai, H.Z., Pan, Z.P.: BDS3/GPS system basic analysis. In: The 10th China Satellite Navigation Annual Conference pp. 5 (2019)
18. Hu, C., Wang, Z.Y., Wang, Q.X., et al.: An improved model for inter-system bias estimation based on BDS-2/BDS-3 combined precise orbit determination. J. Wuhan Univ. Inf. Sci. Ed. **46**(03), 360–370 (2021)
19. Song, M.H., Chai, Y.J., Zhang, B.C.: Analysis on characteristic of inter-system bias between GPS/BDS and its impact on PPP. J. Navig. Positioning **8**(06), 46–52 (2020)
20. He, Y.L.: Research on System Deviation Modeling and Forecasting Methods among Multiple GNSS. China University of Mining and Technology (2019)